Physica Medica 31 (2015) 72–79

Contents lists available at ScienceDirect

Physica Medica

journal homepage: http://www.physicamedica.com

Technical notes

Quantitative comparison between the commercial software STRATOS® by Philips and a homemade software for voxel-dosimetry in radiopeptide therapy

E. Grassi [a, *], F. Fioroni [a], V. Ferri [a], E. Mezzenga [a], M.A. Sarti [a], T. Paulus [c], N. Lanconelli [d], A. Filice [b], A. Versari [b], M. Iori [a]

[a] Medical Physics Dept., IRCCS – S. Maria Nuova Hospital, Viale Risorgimento 80, I-42123 Reggio Emilia, Italy
[b] Nuclear Medicine Dept., IRCCS – S. Maria Nuova Hospital, Viale Risorgimento 80, I-42123 Reggio Emilia, Italy
[c] Philips Technologie GmbH Innovative Technologies, Pauwelsstr. 17, 52074 Aachen, Germany
[d] Dept. of Physics, University of Bologna, I-40126 Bologna, Italy

ARTICLE INFO

Article history:
Received 10 December 2013
Received in revised form
2 October 2014
Accepted 5 October 2014
Available online 25 October 2014

Keywords:
Dosimetry
Voxel
Dose distribution
DVH
Radionuclide therapy

ABSTRACT

Background: Targeted radionuclide therapy is a rapidly growing modality. A few commercial treatment planning systems are entering the market. However, some in-house systems are currently developed for a more flexible and customized dosimetry calculation at voxel-level. For this purpose, we developed a novel software, VoxelMed, and performed a comparison with the software STRATOS.
Methods: The validation of both of them was undertaken using radioactive phantoms with different volume inserts. A cohort of 10 patients was also studied after a therapeutic administration of ^{177}Lu-labelled radiopeptides. The activity, number of disintegrations, absorbed dose and dose-volume histogram (DVH) were calculated for the phantoms and the kidneys in patients, which were the main critical organs at risk in this study.
Results: In phantoms the absorbed doses computed with VoxelMed and STRATOS agree within 5%. In patients at the voxel-level the absorbed dose to kidneys (VoxelMed: mean 0.66 Gy/GBq) showed a limited difference of 5%, but with a remarkable range (−40%, +60%) between the two software packages. Voxel-dosimetry allows to estimate the dose non-homogeneities in volumes, which may be evaluated through DVHs.
Conclusion: This study demonstrates that a fully 3D voxel-dosimetry with multiple SPECT images is feasible by using home-made or commercial software package and absorbed dose results obtained are similar. The main difference between the studied tools was observed in the activity integration method (effective vs physical half-time to time activity curve tail). We believe that an effective half-time integration method produces a more accurate approximation of clinical uptake and resultant dosimetry.

Introduction

In the last decade, peptide receptor radionuclide therapy (PRRT) with somatostatin analogues has been increasingly used for the treatment of metastasized neuroendocrine tumours. On the other hand patient-specific dosimetry can provide information to assess both organ-specific and tumour absorbed doses, and to avoid healthy organ toxicity [1]. An accurate dosimetry is so necessary to understand the radiobiological considerations that affect treatment response [2]. Different dosimetric methods can be applied. They are generally based on the MIRD (Medical Internal Radiation Dose) indications.

The MIRD scheme [3] may be employed through either hybrid (3D SPECT plus serial planar) or fully 3D SPECT-CT-based dosimetry. Organ and equivalent dose values may be then calculated with MIRDose or the OLINDA/EXM software (Vanderbilt University, Nashville, USA).

MIRD no. 23 [4] describes a voxel-level approach, in which the absorbed dose is computed at voxel-level, accounting for the non-uniformity at a maximum level of detail accessible *in vivo*. This produces dose-volume-histograms (DVHs) and radiobiological parameters of great interest for radionuclide therapy.

The voxel-based methods are not widely used in clinical practice and only two commercial software packages are available:

* Corresponding author. Tel.: +39 0522 296937; fax: +39 0522 296392.
E-mail address: elisa.grassi@asmn.re.it (E. Grassi).

http://dx.doi.org/10.1016/j.ejmp.2014.10.002
1120-1797/

STRATOS (Philips Technologie, Aachen, Germany) [11] and VoxelDose (DosiSoft, Cachan, France) [5].

Despite this, for a more flexible and customized dosimetry calculation at voxel-level, in-house software packages were developed by many groups, using 3D information from PET/CT or SPECT/CT [6,7].

The aim of the present work is to compare the results obtained with two different software packages for voxel-dosimetry when processing the same image sets: 1) the software package VoxelMed (VM) developed at our institute; 2) the STRATOS research module.

Material and methods

Phantoms

All activity measurements were performed with an accurate activity calibrator (Aktivimeter Isomed 1010, Nuklear Medizintechnik, Germany), specifically calibrated for ^{177}Lu measurements. All phantoms features are summarized in Table 1.

All phantoms were acquired through a SPECT-CT scanner (Symbia T2, Siemens Medical, Germany, 3/8" NaI(Tl)-detector). The energy windows (EW) of ^{177}Lu photopeaks were set at 113 keV ± 7.5% and 208.4 keV ± 7.5%. For the lower EW, the TEW scatter correction was employed (lower scatter window 87.58 − 104.53 keV, weight = 0.5; the upper scatter window 121.47 − 130.51 keV, weight = 0.9375). For the higher EW, the DEW scatter correction was employed (lower scatter window 171.60 − 192.40 keV, weight = 0.75).

Two cylindrical phantoms were used. The home-made 'Phantom-B' was filled with a homogeneous radioactive solution of ^{177}Lu, while 'Phantom-D' (Data Spectrum Corporation, USA) was provided with six spheres filled with a ^{177}Lu solution in a hot background.

'Phantom-D' was acquired with the standard clinical SPECT-CT protocol for brain studies.

It was used to study the accuracy and the distribution of the activity (A), number of disintegration (ND) and absorbed dose (D) at the voxel-level in the ideal case of only physical decay, at 5, 164, 333 and 500 h after phantom preparation.

'Phantom-B' was acquired with the standard clinical SPECT-CT protocol for body studies.

It was used to study the accuracy and the distribution of the dosimetric values A, ND and D at the voxel-level. The acquisition of the phantom in air was repeated 5 times (30 min, 4 h, 24 h, 48 h and 60 h after injection) at activity concentrations that were intended to simulate a clinical time activity curve.

To extrapolate a single calibration factor CF (expressed in Bq/counts unit, i.e. independent on voxel size of images) shared by both voxel-dosimetry tools, the cylindrical plastic 'Phantom-A' (Data Spectrum Corporation, USA) and 'Phantom-C' (that is 'Phantom-D' essentially without inserts), were filled with a homogeneous ^{177}Lu solution.

The absolute CF for body protocol was determined from 'Phantom-A' (0.065 MBq/ml), while for brain protocol it was determined from 'Phantom-C' (0.40 MBq/ml).

Multiple volumes of interest (VOIs) were manually drawn on one of the CT images and the total counts were extrapolated from the corresponding SPECT images for each object inside the phantoms and for each phantom.

The SPECT-CT scanner was characterized for PVE (Partial Volume Effect) by extrapolation of recovery curves for ^{177}Lu, as a function of volume. All data (A; ND/A and D/A, that are ND and D ratio to activity A), were shown already corrected for PVE.

Acquisition and reconstruction clinical protocols

The standard Siemens clinical protocol for brain studies used: two MEHR collimators; matrix = 128 × 128; zoom = 1.23; views = 60 × 2; time/view = 30 s; step and shoot mode; degree of rotation = 180°; non-circular orbit; detector configuration = 180°. The SPECT projections were reconstructed by an iterative algorithm with compensations for attenuation from CT images, scatter, and full collimator-detector response in Siemens E-Soft workstation (Flash 3D iterative algorithm: 12 iterations; 8 subsets; gaussian filter cut-off = 3.9 mm; 3.9 mm cubic voxel for brain protocol).

Table 1
Description of phantoms used in the study.

Acquisition protocol	Index	Picture	Vol. (ml)	Geometry h = height d = diameter	Insert (ml)	Aim	Activity concentration (MBq/ml)
Body	A	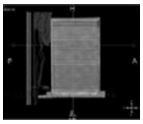	9580	Cylinder h:30, d:20 (internal values)	–	CF calculation	homogeneous solution: 0.065
	B	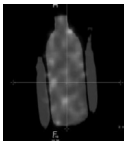	500	Plastic bottle + water bags h:18, d:6	–	effective decay test	refilled homogeneous solution (× 10^{-3}): 2.2, 2.7, 1.89, 0.94, 0.13
Brain	C	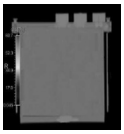	5640	Jaszczak Cylinder (no insert) h:18, d:21 (internal values)	–	CF calculation	homogeneous solution: 0.40
	D	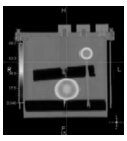	5640	Jaszczak Cylinder (personalized inserts) h:18, d:21 (internal values)	7 fillable spheres (98, 26.5, 19, 11.5, 5.6, 2.57) + extruded polystyrene foam support	test CF and physical decay test	hot background: 0.38, spheres:3.44

The standard Siemens clinical protocol for body studies used: two MEHR collimators; matrix = 128 × 128; zoom = 1; views = 32 × 2; time/view = 30 s; step and shoot mode; degree of rotation = 180°; non-circular orbit; detector configuration = 180°. The SPECT projections were reconstructed by an iterative algorithm with compensations for attenuation from CT images, scatter, and full collimator-detector response in Siemens E-Soft workstation (Syngo, MI Application version 32B, Siemens Medical Solution, Germany) with Flash 3D iterative algorithm (10 iterations; 8 subsets; gaussian filter cut-off = 4.8 mm; 4.8 mm cubic voxel for body protocol).

These reconstructed images were the starting point of both voxel-dosimetry tools.

Patients

A cohort of 10 patients was enrolled in the radiolabelled peptide therapy (^{177}Lu-DOTATATE) in the period 2010-2011 (EUDRACT-Number 2008-000983-17; 2006-000897-65). Patients gave written informed consent. They are different in sex and age (4 females, 6 males, mean age = 65.4, range = 48–79yrs). The adopted administration protocol was described in Ref. [8].

After a therapeutic administration of ^{177}Lu-labelled peptides with renal protection (mean administered activity per cycle was 5.7 ± 1.2 GBq), all patients underwent a series of SPECT-CT scans of the abdomen, at 1, 4, 24, 44, 72 h p.i., with the standard clinical acquisition protocol for body studies. No particular method for assuring reproducibility of patient positioning in subsequent imaging was adopted: patients were positioned in supine configuration with arms raised and placed on a shaped pillow.

Dose calculation of only critical organs (kidneys) was performed. Mean dose computation of these organs using the OLINDA/EXM package was also performed and considered as a reference.

The same sets of images were evaluated with STRATOS and VoxelMed.

VoxelMed

This software package was designed on CERR version 4.0 (www.cerr.info).

VoxelMed (VM) allows users to:

1. perform a manual segmentation of VOIs on the CT image and automatically copy them on all the imported SPECT slices;
2. calculate ND distribution at voxel-level for each VOI;
3. calculate the 3D dose distribution as a result of the convolution between the ND matrix and the *S*-values matrix (both beta and gamma contribution) for therapy isotope;
4. compute DVH and dose statistics in each VOI;

SPECT images were exported from Siemens workstation already aligned to the first CT image through a manual rigid registration. The registration tools provided by Siemens rescaled the original voxel size to 3.9 × 3.9 × 3.5 mm and to 2.32 × 2.32 × 2 mm for body and brain studies, respectively.

Voxel-*S*-values specific for the voxel sizes considered in the study were simulated by the University of Bologna (www.medphys.it) [9].

In order to compute the value of ND at the voxel-level, VoxelMed was designed to apply the trapezoidal method up to the last time acquisition point [that is, no tail contribution to total integral, referred as VM(no tail)] plus an effective half-life exponential analytical integral, as a mono-exponential tail contribution from the last time acquisition point onwards [referred as VM(eff)]. The effective half-time used for tails was derived from the exponential fitting (least squares analysis) of the whole time–activity curve in each VOI. The tail integral was calculated on this effective mono-exponential starting from the last acquisition point onwards. Integral of tails after the last point represents a large proportion of the total integral. This choice for tails was supported by Ref. [10] for organ level dosimetry.

VoxelMed was also designed to use the trapezoidal integration method up to the last time point, plus a physical half-life integral for tail [referred as VM(phys)], similarly to the technique employed by STRATOS.

STRATOS

This commercially available product for voxel-based dosimetry is part of the IMALYTICS Research Workstation.

The software package is based on the MIRD formalism for voxel-based dose calculation by voxel-*S*-values. The complete workflow used to analyse the set of 3D images allows users to do the same as points 1, 2, 3, 4 of VoxelMed [11]. SPECT images instead were aligned to the first CT image through a rigid registration in STRATOS workstation.

Since voxel-*S*-values depend on the isotope and on the voxel size of the grid, orginal activity images (4.8 mm cubic size) were resampled in STRATOS to voxels of 4.42 × 4.42 × 4.42 mm in accordance with STRATOS' voxel-*S*-value sizes. Creating and using new voxel-*S*-values for different voxel-sizes is now supported in collaboration with the company.

To calculate the ND, the software package by default applies the trapezoidal integration method plus a physical half-time mono-exponential tail integration after the last time point.

Other calculation options (analytical integration of fitted data or using effective half-times) may be currently available only after editing configuration files and in collaboration with the company.

OLINDA/EXM

The same sets of images used in voxel-dosimetry calculation were used for dosimetry at organ level. VOIs were drawn manually on all CT images by the software Volumetric Analysis in Siemens E-soft workstation.

The estimates of the dose to critical organs were obtained by OLINDA/EXM software package, mentioned as OLINDA in the following. Patient-specific organ masses were also considered.

For phantom analysis, the OLINDA sphere model tool was applied based on the known injected activity in the inserts, rather than using image data.

Comparison of software

The consistency between the analysed tools was evaluated in terms of relative difference (R) of volume, mean A quantification inside VOIs, mean ND/A per voxel, and D/A in VOIs in both phantoms and patients.

Being X the quantity to be studied and X_{ref} the quantity chosen as a reference, the quantity R was defined as:

$$R = ((X - X_{ref})/X_{ref})*100$$

In phantoms, the quantity X to be studied was derived from original data. Reference X_{ref} values came, instead, from phantom/insert defined volume, activity measurements in activity calibrator, while the reference for ND/A and D/A were computed with OLINDA/EXM sphere model (ND/A and D/A were normalised to voxel size; while activity and volume values were referred to the whole VOI).

In case of VoxelMed and STRATOS, the values of A, ND/A, and D/A were derived from image analysis. In both 'Phantom-D' and 'Phantom-B' ND/A are calculated by trapezoidal method on serial images up to the last time point and physical decay in the tail up to 500 h post injection.

In ND/A and D/A computation, X_{ref} was considered as the organ level value provided by OLINDA, then normalized to the voxel size, while X was the value provided by STRATOS, VM(phys) or VM(eff).

Statistical analysis was performed through the nonparametric two-tailed Wilcoxon test (significance level 0.05) designed to evaluate the difference between two matched samples (ND/A and D/A absolute values in kidneys) with a limited number of data. The null hypothesis was that the medians of the two samples were identical. The p-values are reported in results section.

For both phantoms and patients, results for ND/A and D/A were provided as an average over voxels inside volumes for both voxel-dosimetry and OLINDA techniques. The analysis of the coefficients of variation inside volumes, CV, defined as the ration between the standard deviation and the mean value of a series of data, was performed to measure fluctuations among voxels for ND/A and D/A.

Results

Phantoms results

The calibration factor for both voxel-dosimetry methods was obtained from the ratio between the activity content (MBq/ml) and the mean counts in images (counts/ml): 26 Bq/counts ('Phantom-A') and 13 Bq/counts ('Phantom-C') for body and brain studies, respectively.

Measured volumes of VOIs by STRATOS and VoxelMed are shown in Table 2 for both 'Phantoms-D' and 'B'. They are used to test voxel methods on body and brain protocols, respectively.

Table 3 shows R values for A, ND/A (X_{ref} are OLINDA values from exponential fitting) and D/A (X_{ref} are OLINDA values from sphere model). X_{ref} for ND/A and D/A is the mean value calculated over all spheres (ND/A = 95 s; D/A = 30.3 Gy/GBq) of 'Phantom-D', while activity refers to the whole activity amount inside each VOI.

Since OLINDA uses activities measured in an activity calibrator, its results are not affected by border effect or by PVE. From ND/A to D/A calculation a general increase of the absolute value of R can be observed, caused by progression of calculation, resulting from error propagation.

Table 4 shows the absolute values for activity in the whole VOI, R and CV for dosimetric values A, ND/A, and D/A in 'Phantom-B' for body acquisition.

In Fig. 1a, the DVHs for phantoms are reported for 98 ml, 19 ml and 5.6 ml spheres and 500 ml cylinder for STRATOS and VoxelMed.

Patients results

The clinical results present kidney estimates. Figure 1b shows the time activity curve interpolation by different techniques: OLINDA, STRATOS, VM(eff) and VM(phys). VM(eff) and VM(phys) are different only on tail side.

Table 6 shows R for VM(phys), VM(eff) and STRATOS. R-values refer to OLINDA ND/A.

The statistical tests performed on ND/A data provided no significant difference between the medians of software packages [STRATOS vs VM(phys) p-value = 0.92; STRATOS vs VM(eff) p-value = 0.85; VM(phys) vs VM(eff) p-value = 0.64]. Nevertheless RMS value is much higher for VM(eff) than for VM(phys) and STRATOS.

Table 7 shows R for STRATOS, VM(phys) and VM(eff). R values are referred to OLINDA D/A.

The statistical tests performed on data provided no significant difference between STRATOS and VM(phys) (p-value = 0.64) and STRATOS vs VM(eff) (p-value = 0.17), while VM(phys) vs VM(eff)

Table 2
Measured volume results in 'Phantom-D' and 'Phantom-B'.

Volume (ml)	Real value	STRATOS	VM	R STRATOS (%)	R VM (%)
Phantom D	98.00	100.50	100.32	2.6	2.4
	26.50	28.80	28.57	8.7	7.8
	19.00	18.00	17.09	−5.3	−10.1
	11.50	10.70	12.98	−7.0	12.8
	5.60	6.90	6.41	23.2	14.4
	2.57	2.80	2.98	8.9	15.9
mean	–	–	–	9.8	10.5
Phantom B	500.00	532.00	471.00	6.40	−5.8

Table 3
'Phantom-D' results.

	Volume (ml)	R STRATOS (%)	R VM(phys) (%)	CV STRATOS (%)	CV VM(phys) (%)
A	98	−5.4	−5.3	30.1	28.8
	26.5	2.8	4.7	42.8	44.6
	19	−9.9	−5.7	36.1	35.2
	11.5	−5	7.4	38.2	40
	5.6	8.8	9.2	37.4	40.5
	2.57	−3.9	−2.5	28.5	29.8
mean		2.1	1.3	35.5	36.5
RMS		6.5	6.2	–	–
ND/A	98	−2	−0.4	56.7	57.2
	26.5	−10.2	−6.2	55.8	60.0
	19	−0.7	−0.9	56.5	61.4
	11.5	−1.5	−7.2	56.8	53.7
	5.6	−18.6	−12.1	57.6	58.2
	2.57	−13.7	−11.3	43.8	62.2
mean		−7.8	−6.4	49.3	58.5
RMS		10.4	7.8	–	–
D/A	98	−4.8	−4.3	26.2	51.4
	26.5	−12.7	−11.8	47.5	54.7
	19	−3.9	−5.3	50.3	58.4
	11.5	−0.1	−6	45.6	47.7
	5.6	−20.9	−19.2	49.2	53.8
	2.57	−15.6	−18	37.0	39.9
mean		−9.7	−10.8	41.9	49.1
RMS		12.1	12.3	–	–

Table 4
'Phantom-B' results.

	OLINDA	STRATOS		VM(phys)	
	Absolute value	R(%)	CV(%)	R(%)	CV(%)
A	1103 KBq	−3	56	−13	55
ND/A mean voxel	42 s	−15.1	43	−14.3	42
D/A	7.4 Gy/GBq	−18.9	42	−20.9	40

Table 5
Inaccuracy analysis for 'Phantom-D' and 'Phantom-B'.

	Brain (phantom D)		Body (phantom B)		Mean
	STRATOS (%)	VM(phys) (%)	STRATOS (%)	VM(phys) (%)	
Volume delineation	9.3	10.6	6.4	5.8	8
Activity quantification	2.1	1.3	3	10	4.1
Fitting	5.7	5.1	12.1	4.3	6.8
Dose	1.8	3.8	3.8	6.6	4
Quadratic summation	11.3	12.4	14.5	14.0	11.9

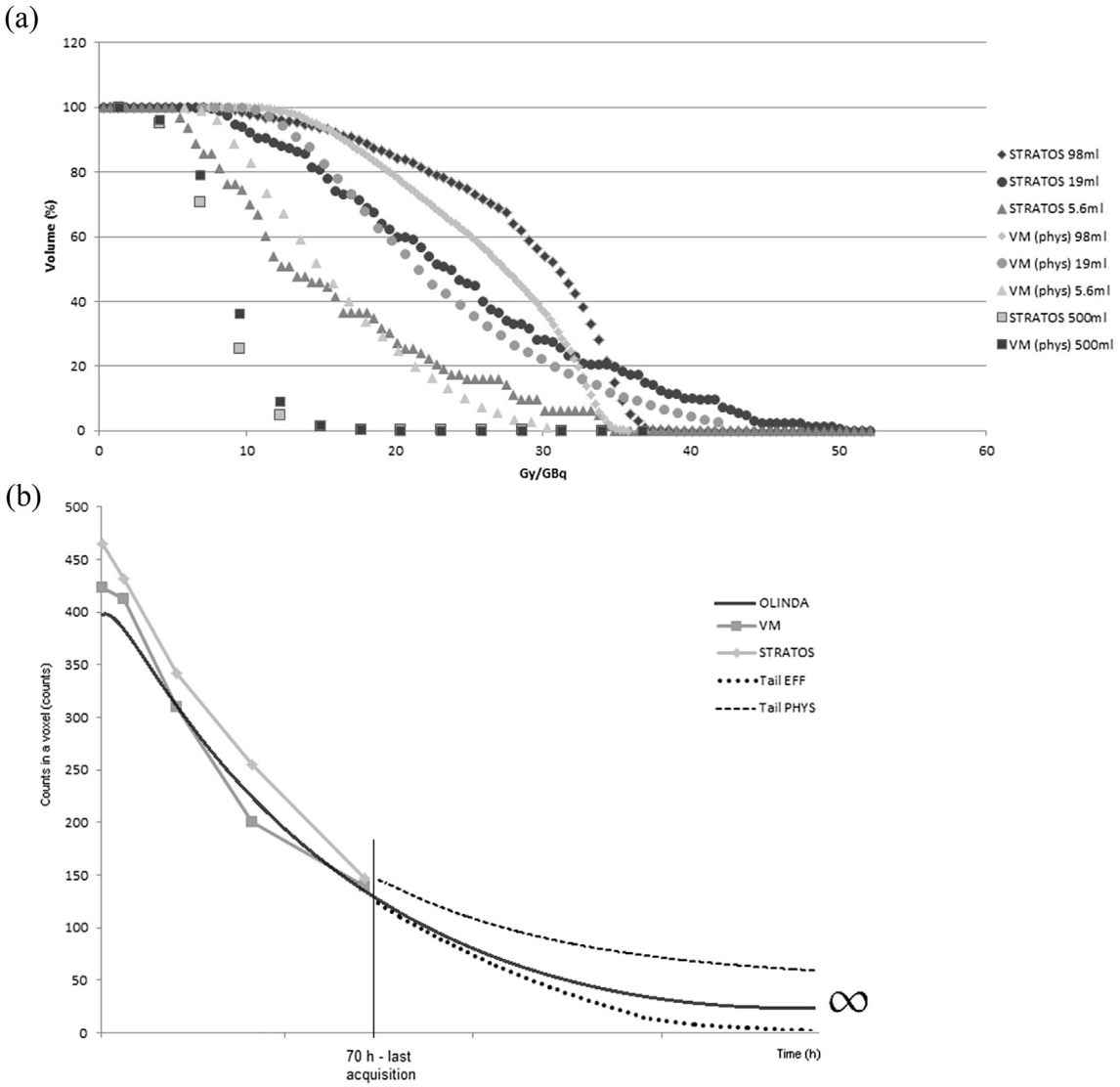

Figure 1. a) DVH for 'Phantom-D' inserts and 'Phantom-B'; b) time activity curve differently interpolated.

showed a significant difference (p-value = 0.005) between medians of the two samples. In this case the RMS value for VM(eff) is higher than VM(phys) and STRATOS, which are instead close to each other.

Figure 2a shows DVH for patient-1, whose values for right kidney dose estimates by STRATOS and VM(phys) were very close, while Fig. 2b shows a DVH for patient-6, whose values for right kidney dose estimates by STRATOS and VM(phys) were far from each other.

In the same Figure, right kidney DVH for patients-1 and -6 are also shown for VM(eff) results.

Figure 3 reports VoxelMed DHV for patient-7 and patient-9 for VM(phys), VM(eff), and VM(no tail) results, to focus attention on different tail contribution in dose estimation.

Table 6
ND/A patient results averaged on both kidneys.

ND/A	R(%) STRATOS	R(%) VM(phys)	R(%) VM(eff)
pt1	−19	−11.5	−20
pt2	−2.3	9	−36.5
pt3	−55	−54.2	−55
pt4	14.6	18	48.4
pt5	−11	−23.6	−36.2
pt6	−6.9	−19	−52.3
pt7	22.2	14.8	−45.9
pt8	18	12	−19.3
pt9	−15.8	−19.7	−44.2
pt10	−12.3	−12.1	−32.3
RMS	22.3	23	40.8
st−dev	22.4	22.5	29.8

Table 7
D/A patient results averaged on both kidneys.

D/A	R(%) STRATOS	R(%) VM(phys)	R(%) VM(eff)
pt1	14.9	12.7	−29.2
pt2	28.9	26.7	16.4
pt3	18.0	−40.8	−42.1
pt4	−12.7	28.0	20.1
pt5	7.0	−13.3	−32.2
pt6	11.1	−15.8	−35.3
pt7	−25.3	−8.1	−37.8
pt8	−32.0	−30.5	−38.8
pt9	−0.8	−11.4	−22.2
pt10	22.5	12.4	3.3
RMS	**19.7**	**22.4**	**30.0**
st−dev	**9.9**	**10.7**	**12.1**

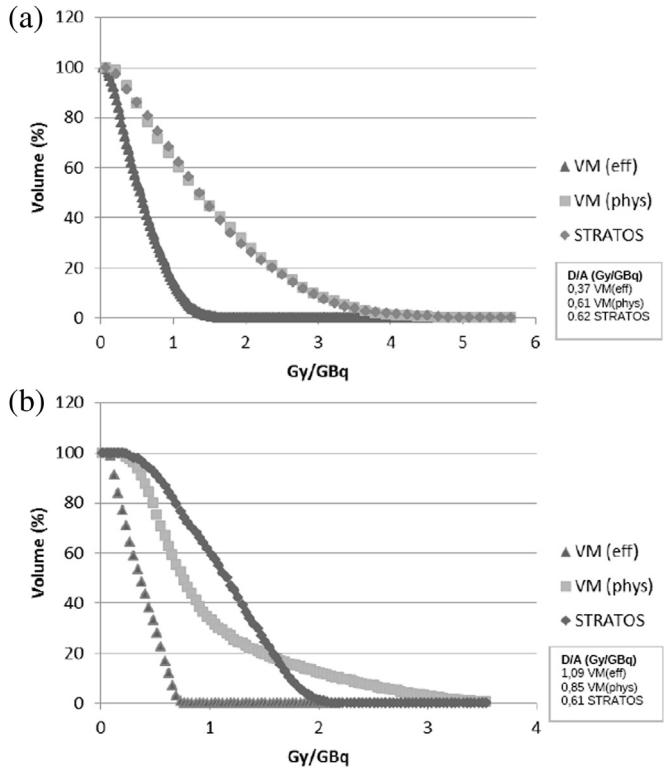

Figure 2. (a) patient-1; (b) patient-6 kidney DVH.

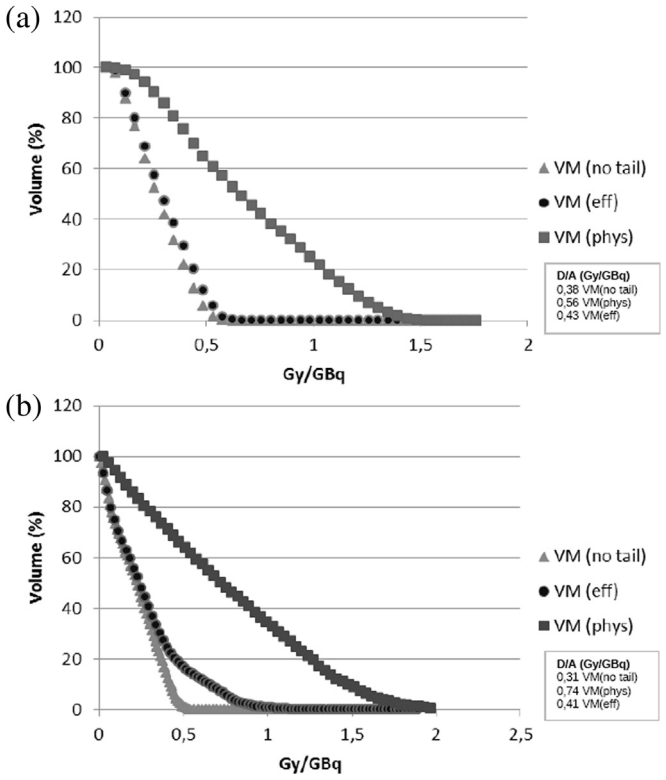

Figure 3. (a) patient-7; (b) patient-9 kidney VoxelMed DVH.

Figure 4 shows the steps in dosimetric voxelized calculation with VoxelMed: kidneys contouring on CT scan, registered SPECT image and finally the dose distribution in kidneys.

Discussion

The aim of the present work was to compare two tools for voxel-based dose calculation on phantoms and on clinical cases. The starting images were the same in both cases, but the dosimetry calculations were performed independently, with the double aim of testing the reproducibility deriving from either software packages and the effect of time activity curve tail integration technique.

Phantoms

The first encountered cause of error in quantification is volume inaccuracy in the contouring phase for both approaches. This difference was estimated through the defined quantity *R*. It was independent of sphere size in 'Phantom-D', while about 6% in 'Phantom-B' (Table 2). STRATOS and VoxelMed show good agreement in this first step.

These deviations, though not large, could be attributed to: different voxel size of images; image alignment (manual/automatic rigid registration) and diverse contouring performed independently in VoxelMed and STRATOS workstation; interoperator variability.

The inaccuracy in activity estimates, shown in Tables 3 and 4, derives from different sources, such as those previously mentioned about volume bias.

In ND/A sphere estimates (Table 3) the two methods show a variation (mean and RMS values) within a few-percent between each other when the same tail integration method is applied.

In case of 'Phantom-B' (Table 4), *R* values for ND/A are in general higher than 'Phantom-D' sphere values. The activity values for 'Phantom-D' are based solely on physical decay. This may represent an 'easier' situation for fitting time activity curves by the tested software packages. The CV for ND/A inside spheres do not show a strong dependence on sphere size (Table 3). STRATOS values are slightly lower than those obtained with VM(phys), while in Table 4 they are very close.

In the absorbed dose computation of 'Phantom-D' and 'Phantom-B' (Tables 3 and 4 respectively), an underestimation is evident compared to OLINDA.

The results for Phantom-D' and 'Phantom-B' are different because most likely the reference geometry is a sphere model. It introduces a bias for 'Phantom-B', which isn't a sphere and in practice will have a larger escaping fraction due to its relatively higher surface area.

A DVH (Fig. 1a) analysis of 'Phantom-D' showed that values for STRATOS and VoxelMed were very close to each other, as in Table 3. The 'Phantom-B' DVHs closely overlap, as in Table 4. To some extent, DVHs are affected by PVE, uncertainties in image alignment and heterogeneities in tissue density/composition, noise and resolution in SPECT imaging [12].

Phantom analysis provided a global inaccuracy in either software of approximately 12%, achieved by summing the single sources of errors (Table 5) for both phantoms.

In clinical cases, where a higher inaccuracy is expected to more complicated biological pharmacokinetics *in vivo*, an error in dose estimation may exceed 12%.

Patients

There is a great inter-patient variability in results for both tools (Tables 6 and 7), even though the mean results show a reasonable agreement.

ND/A results for VM(phys) are closer to STRATOS ones than VM(eff), as seen in *R* values in Table 6. Statistical analysis indicated

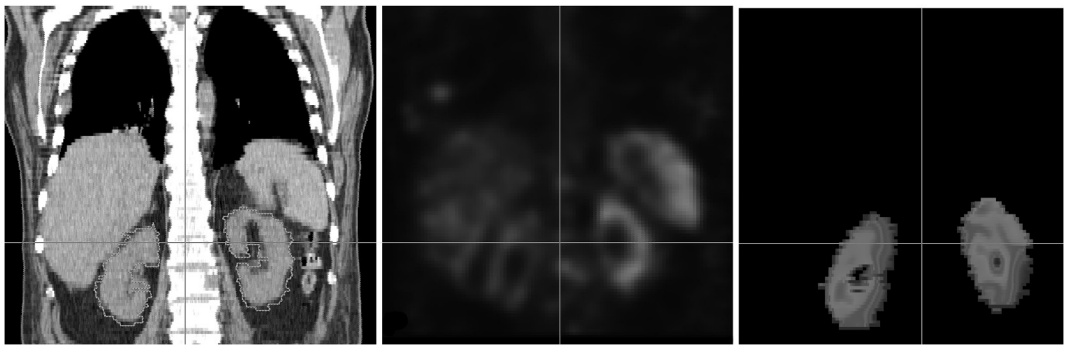

Figure 4. VoxelMed coronal image set: CT scan with structure, first SPECT scan and dose map.

no significant difference between the software packages [STRATOS vs VM(phys) and STRATOS vs VM(eff)].

The standard deviations for ND/A show considerable inter-patient variability, but no strong dependence on the adopted method (Table 6).

Results for D/A (Table 7) show high inter-patient variability too.

Wilcoxon test showed that only VM(phys) and VM(eff) were significantly different, while STRATOS was not vs either of them. VM(phys) and VM(eff) are different because diverse tail integration methods are applied, whereas trapezoidal method is applied. Nevertheless, p-values for STRATOS vs VM(eff) ($p = 0.17$) were much lower than STRATOS vs VM(phys) ($p = 0.64$), although the first comparison result was not significantly different. This provide some evidence that STRATOS and VM(phys) are more strongly connected, as expected, as they share the same schema, despite the difference in image alignment which affects the comparison. The same is evident also in RMS values, that are higher for VM(eff) than for STRATOS and VM(phys).

In Fig. 2b, DVH curves do not overlap, as expected from R values in Table 7.

This underlines the importance of considering dose distribution in place of an average organ level approach. In particular in the integration with external radiotherapy this aspect has been becoming nowadays much more important.

In Fig. 2a, instead, the curves for STRATOS and VM(phys) overlap. In both cases, their DVHs are far from VM(eff) DVH, which is more likely since it applies the effective decay tail.

The sharp slope of the VM(eff) DVH in Fig. 2 indicates a lower variability in dose distribution, compared to VM(phys).

Looking at VM(no tail) and VM(eff) DVHs for patients in Fig. 3, the variability in activity uptake among patients after the last point is evident: patient 7's DVHs (Fig. 3a) don't show marked differences, while in Fig. 3b, patient 9's DVHs indicate that activity was still present after the last time point acquisition. Furthermore the difference between VM(eff) and VM(phys) is evident in Fig. 3, in both patients.

Caused by a major homogeneity in tail integral contribution to ND/A, the strong weight of tails compared to the total integral is estimated in about 70% for trapezoidal integration method plus physical decay after last time point, while 40% for effective decay, as in Ref. [13]. This aspect influences the D map calculation.

The ratio between the mean D/A values for VM(eff) and VM(phys) is 45% for patient 9 and 55% for patient 7. Again this indicates a large contribution from the tail portion of the total integral in VM(phys). Since phantom analysis indicated a global inaccuracy of about 12% (Table 5), in clinical cases another 20 to 30% uncertainty may be expected for both voxel-dosimetry tools.

Concluding, OLINDA is a good reference for comparison between different models, though based on an organ level computation. VM(eff) shows a slight tendency to underestimate cumulated activity and D/A values compared to STRATOS and VM(phys). An effective half-time approach is probably more reliable for estimating time activity curves for voxel-based dosimetry. A physical half-time tail integration doesn't maximize patient-specific information, as effective half-time model instead does being more biologically accurate [13], and almost certainly overestimates absorbed dose calculation.

When comparing different dosimetric methods the integral technique and preparation of images for dosimetry computation must both be considered. It is also reminded that all internal dosimetry software calculation methods should be evaluated according to the EANM guidelines [14], prior to implementation in clinical routine.

Seen the differences that may arise from the application of these two innovative tools, it is recommended to deserve deep attention in validation of new codes for voxel dosimetry, especially if issues about realignment of subsequent scans and fitting can be recognized.

Conflict of interest

Dr. Timo Paulus is Business Manager Director of Philips Technologies, Research Laboratories (Germany) and kindly made Imalytics Research Workstation available to our centre for data elaboration.

Acknowledgements

Authors are grateful to Dr. Nico Lanconelli, University of Bologna, for the meaningful support in computation of specific voxel-S-values and the suggestions about developing VoxelMed.

Authors appreciate also the kind scientific suggestions and English editing revision of Dr. Nick Patterson, Velindre Cancer Centre, Cardiff (UK).

References

[1] Zaknun JJ, Bodei L, Mueller-Brand J, Pavel ME, Baum RP, Hoersch D, et al. The joint IAEA, EANM, and SNMMI practical guidance on peptide receptor radionuclide therapy (PRRNT) in neuroendocrine tumours. Eur J Nucl Med Mol Imaging 2013;10. 1007/s00259-012-2330-6.

[2] Strigari L, Benassi M, Chiesa C, Cremonesi M, Bodei L, D'Andrea M. Dosimetry in nuclear medicine therapy: radiobiology application and results Q. J Nucl Med Mol Imaging 2011 Apr;55(2):205–21.

[3] Siegel JA, Thomas SR, Stubbs JB, Stabin MG, Hays MT, Koral KF, et al. MIRD pamphlet No 16: techniques for quantitative radiopharmaceutical biodistribution data acquisition and analysis for use in human radiation dose estimates. J Nucl Med 1999;40:37S–61S [MIRD Supplement].

[4] Dewaraja YK, Frey EC, Sgouros G, Brill AB, Roberson P, Zanzonico PB, et al. MIRD pamphlet No. 23: quantitative SPECT for patient-specific 3-dimensional

dosimetry in internal radionuclide therapy. J Nucl Med 2012 Aug;53(8):1310–25.
[5] Dieudonné A, Garin E, Laffont S, Rolland Y, Lebtahi R, Leguludec D, et al. Clinical feasibility of fast 3-dimensional dosimetry of the liver for treatment planning of hepatocellular carcinoma with 90Y-microspheres. J Nucl Med 2011 Dec;52(12):1930–7. http://dx.doi.org/10.2967/jnumed.111.095232. Epub 2011 Nov 8.
[6] Grimes J, Uribe C, Celler AJADA. A graphical user interface for comprehensive internal dose assessment in nuclear medicine. Med Phys 2013 Jul;40(7). http://dx.doi.org/10.1118/1.4810963. 072501.
[7] Jackson PA, Beauregard JM, Hofman MS, Kron T, Hogg A, Hicks RJ. An automated voxelized dosimetry tool for radionuclide therapy based on serial quantitative SPECT/CT imaging. Med Phys 2013;40(11). 112503/1–112503/8.
[8] Sghedoni R, Grassi E, Fioroni F, Asti M, Piccagli V, Versari A, et al. Personnel exposure in labelling and administration of (177)Lu-DOTA-D-Phe1-Tyr3-octreotide. Nucl Med Commun 2009 Feb;30(2):176–82.
[9] Lanconelli N, Pacilio M, Lo Meo S, Botta F, Di Dia A, Torres Aroche LA, et al. A free database of radionuclide voxel S values for the dosimetry of non uniform activity distributions. Phys Med Biol 2012;57:517–33.
[10] Traino AC, Marcatili S, Avigo C, Sollini M, Erba PA, Mariani G. Dosimetry for non uniform activity distributions: a method for the calculation of 3D absorbed-dose distribution without the use of voxel S-values, point kernels, or Monte Carlo simulations. Med Phys 2013;40(4).
[11] Berker Y, Goedicke A, Kemerink GJ, Aach T, Schweizer B. Activity quantification combining conjugate-view planar scintigraphies and SPECT/CT data for patient-specific 3-D dosimetry in radionuclide therapy. Eur J Nucl Med Mol Imaging 2011;38:2173–85.
[12] Cheng L, Hobbs RF, Segars PW, Sgouros G, Frey EC. Improved dose-volume histogram estimates for radiopharmaceutical therapy by optimizing quantitative SPECT reconstruction parameters. Phys Med Biol 2013 Jun 7;58(11):3631–47.
[13] Guerriero F, Ferrari ME, Botta F, Fioroni F, Grassi E, Versari A, et al. Kidney dosimetry in 177Lu and 90Y peptide receptor radionuclide therapy: influence of image timing, time-activity integration method, and risk factors. Biomed Res Int 2013;2013:935351. http://dx.doi.org/10.1155/2013/935351. Epub 2013 Jun 20.
[14] Lassmann M, Chiesa C, Flux G, Bardiès M. EANM dosimetry committee guidance document: good practice of clinical dosimetry reporting. Eur J Nucl Med Mol Imaging 2011;38:192–200.